



WULoc: Achieving Extremely Long-range High-precision Localization via Wi-Fi-UWB Connection

KAI SUN*, Southeast University, China

SHUAI WANG*, Southeast University, China

RENJIE ZHAO, The Johns Hopkins University, United States

RUOFENG LIU, Michigan State University, United States

WEIWEI CHEN, Shanghai University, China

ZHIMENG YIN, City University of Hong Kong, CityU HK Shenzhen Research Institute, China

WEI GONG, University of Science and Technology of China, China

SHUAI WANG[†], Southeast University, China

Wireless localization, especially using ubiquitous Wi-Fi devices, has been studied for decades. However, due to complex signal propagation, resolving multiple reflected paths and further achieving accurate localization face great challenges in the localization precision and localization range, which are caused by the limited bandwidth and sensitivity of Wi-Fi signals respectively. Straightforwardly solving these challenges by employing wide bandwidth Wi-Fi is only helpful for improving precision, while the localization range is still short due to Wi-Fi's intrinsic vulnerability to SNR drop. This paper presents Wi-Fi-UWB Localization (WULoc) to achieve both precise and long-range localization for Wi-Fi devices. Specifically, WULoc leverages the picosecond level timestamp information that is extracted from the links of the Wi-Fi device to multiple UWB anchors, innovatively created by the proposed Wi-Fi-UWB connection establishment, which overcomes the incompatibility between Wi-Fi and UWB physical layers. WULoc further calculates the TDoA of Wi-Fi-UWB links, from which the location of the Wi-Fi device is estimated. Extensive experiments show that WULoc locates a Wi-Fi device at a range of 240 meters with a precision of 5.3 meters.

CCS Concepts: • Human-centered computing → Ubiquitous and mobile computing systems and tools.

Additional Key Words and Phrases: Localization, Wi-Fi, UWB, Cross-technology Communication

ACM Reference Format:

Kai Sun, Shuai Wang, Renjie Zhao, Ruofeng Liu, Weiwei Chen, Zhimeng Yin, Wei Gong, and Shuai Wang. 2025. WULoc: Achieving Extremely Long-range High-precision Localization via Wi-Fi-UWB Connection. *Proc. ACM Interact. Mob. Wearable Ubiquitous Technol.* 9, 1, Article 18 (March 2025), 24 pages. <https://doi.org/10.1145/3712282>

* All authors contributed equally to this work.

[†]Corresponding author.

Authors' addresses: Kai Sun, sunk@seu.edu.cn, Southeast University, Nanjing, Jiangsu, China; Shuai Wang, shuaiwang_iot@seu.edu.cn, Southeast University, Nanjing, Jiangsu, China; Renjie Zhao, rjzhao@jhu.edu, The Johns Hopkins University, Baltimore, Maryland, United States; Ruofeng Liu, liuruofe@msu.edu, Michigan State University, East Lansing, Michigan, United States; Weiwei Chen, chenweiwei@shu.edu.cn, Shanghai University, Shanghai, Shanghai, China; Zhimeng Yin, zhimeyin@cityu.edu.hk, City University of Hong Kong, CityU HK Shenzhen Research Institute, Hong Kong, Hong Kong, China; Wei Gong, weigong@ustc.edu.cn, University of Science and Technology of China, Hefei, Anhui, China; Shuai Wang, shuaiwang@seu.edu.cn, Southeast University, Nanjing, Jiangsu, China.

Permission to make digital or hard copies of all or part of this work for personal or classroom use is granted without fee provided that copies are not made or distributed for profit or commercial advantage and that copies bear this notice and the full citation on the first page. Copyrights for components of this work owned by others than the author(s) must be honored. Abstracting with credit is permitted. To copy otherwise, or republish, to post on servers or to redistribute to lists, requires prior specific permission and/or a fee. Request permissions from permissions@acm.org.

© 2025 Copyright held by the owner/author(s). Publication rights licensed to ACM.

ACM 2474-9567/2025/3-ART18

<https://doi.org/10.1145/3712282>

1 INTRODUCTION

Wireless localization has been a prominent research topic for decades. With the emergence of smart cities and smart homes, the need to localize target users has grown significantly to satisfy a diverse range of applications, such as autonomous driving, ridesharing, and navigation. Despite the widespread deployment of the Global Positioning System (GPS) on smartphones and vehicles, GPS precision often degrades in various scenarios, including high-density urban areas with tall buildings [21], tunnels, malls, stadiums, and other environments where the GPS signal level drops. Since these scenarios cover a significant portion of people's daily activities, how to achieve precise localization for target users in these large areas becomes an essential problem.

This paper focuses on exploiting the users' daily carried Wi-Fi devices, such as smartphones and laptops, to achieve long-range and high-precision localization. Given the vast number of Wi-Fi devices and their continuous operation, the ability to localize a Wi-Fi device over a wide range is essential for providing accurate navigation services in areas where GPS coverage may be limited or unreliable [15, 18, 24]. This paper aims to deliver an accurate localization solution for Wi-Fi users that can complement or even surpass the capabilities of GPS-based systems, enabling a more comprehensive cyber-physical system (CPS).

Technically speaking, the existing Wi-Fi localization approaches are unable to deliver both long localization range and high precision at the same time. These approaches utilize Wi-Fi base stations as anchors to estimate the location of the target Wi-Fi device. This estimation is primarily achieved by extracting the time-of-flight (ToF) and angle information from the communication between the target device and the anchor [15, 24, 61]. However, a significant challenge arises when the signal-to-noise ratio (SNR) at the anchors drops considerably, especially in long-range scenarios. Under such conditions, the communication between the target device and the anchors would suffer from excessive noise or even complete failure, resulting in poor localization performance. As validated in the study by [13], the communication performance of 802.11ax degrades by 56% when the distance is 50 meters, and the communication is completely lost at 125 meters in outdoor environments. As designed for high-throughput communication, Wi-Fi employs Orthogonal Frequency-Division Multiplexing (OFDM) as the modulation/demodulation scheme [2], which is inherently sensitive to SNR drop, making the existing Wi-Fi localization approaches unsuitable for delivering both long localization range and high precision simultaneously.

This paper presents WULoc, a novel design to achieve long-range and high-precision localization for Wi-Fi devices. In contrast to the existing Wi-Fi localization approaches that utilize Wi-Fi base stations as anchors, WULoc innovatively allocates the anchors to Ultra-wideband (UWB) devices that operate on the 6 GHz frequency band, overlapping with the Wi-Fi 802.11ax 6E frequency band [6, 39]. By establishing a special communication link from the Wi-Fi target to the UWB anchors, WULoc is able to allow UWB anchors to a precise timestamp from the Wi-Fi-to-UWB communication and calculate the Time Difference of Arrival (TDoA). Subsequently, WULoc applies hyperbolic trilateration to localize the Wi-Fi target based on the TDoA information. WULoc leverages the inherent capabilities of UWB technology to enable both long-range and high-precision localization for Wi-Fi targets. UWB anchors possess an ultra-low SNR signal reception capability [1], which allows them to reliably extract timestamps from the Wi-Fi-UWB communication, even over a long distance. Moreover, marking the shortest path with a high-precision (15.62 picoseconds level) timestamp [1, 39, 41, 44] is a crucial enabler for accurate TDoA calculations, which contribute to achieving precise localization of the Wi-Fi targets.

However, realizing such a long-range and high-precision localization system needs to resolve several **technical challenges**. A key challenge lies in the fundamental incompatibility between the Wi-Fi and UWB physical layers: (i) The modulation schemes for Wi-Fi and UWB are distinct: Wi-Fi employs QAM+OFDM, while UWB uses BPSK+BPM. (ii) Their bandwidths also differ significantly; Wi-Fi typically operates with a maximum bandwidth of 160 MHz, whereas UWB utilizes a much broader 500 MHz signal. This considerable bandwidth gap presents a significant challenge, as Wi-Fi target devices cannot produce a standard 500 MHz UWB signal waveform. (iii) Furthermore, the differences in frame structures between Wi-Fi and UWB add to the complexity. Additionally,

each Wi-Fi symbol includes a cyclic prefix (CP) signal, which is automatically filled and creates further uncertainty in generating UWB-compatible Wi-Fi packets. Another key challenge stems from timestamp information at the UWB anchors. While UWB technology is generally known for its low-cost and simplicity, this simplified circuit design of low-cost UWB implementations often leads to unstable local oscillators within the UWB anchors. This instability in the oscillator frequency can result in significant jitter in the timestamp data, which in turn degrades the TDoA and location estimation.

To address these challenges, WULoc is built with a series of technical highlights: (i) **Wi-Fi-UWB Connection Establishment** creates reliable communication from the Wi-Fi target to UWB anchors by overcoming the physical-layer incompatibility. Inspired by the recently proposed cross-technology communication (CTC), which enables direct transmission across different wireless technologies without any hardware modification [26, 31, 51], WULoc carefully customizes a Wi-Fi packet so that the transmitted signal can be identified by UWB anchors as a legitimate UWB packet. This is technically achievable due to the signal manipulation capabilities of Wi-Fi, combined with UWB's tolerance for significant signal distortion during demodulation, thereby overcoming the difference in modulation, bandwidth, and frame structure. (ii) **Wi-Fi-UWB TDoA Calculation** presents a periodical calibration mechanism to synchronize the clocks across UWB anchors, thereby obtaining precise TDoA from the picosecond timestamp of the Wi-Fi-UWB transmission. To achieve synchronization among multiple low-cost anchors, WULoc leverages the characteristics of its oscillator variations in the time domain by broadcasting clock alignment packets at a reasonable transmission frequency, minimizing the TDoA errors caused by device differences, and achieving more precise localization. (iii) **Wi-Fi-UWB TDoA based Localization** estimates the localization of the Wi-Fi target via hyperbolic triangulation techniques, which collectively leverages TDoA calculated by UWB anchors. To the best of our knowledge, WULoc is the first-of-this-kind design to achieve long-range and high-precision localization for Wi-Fi devices via Wi-Fi-UWB connection. Upon deployment in real-world scenarios, WULoc is expected to complement existing GPS-based solutions and provide a comprehensive, ready-to-use localization framework for broader CPS applications, ensuring enhanced accuracy and reliability. Our contributions are summarized as follows:

- This paper presents WULoc, the first-of-this-kind system to achieve extremely long-range high-precision Wi-Fi localization via Wi-Fi-UWB connection. The key innovation of WULoc is repurposing existing UWB devices, which have been used for positioning applications, into anchors for localizing Wi-Fi targets over a long distance. The localization capability allows WULoc to become an alternative to GPS in various scenarios, including high-density urban areas with tall buildings, and indoor environments where the GPS service is unavailable.
- Technically, WULoc breaks the communication barrier between the Wi-Fi target and UWB anchors with a carefully designed Wi-Fi-UWB connection establishment mechanism, which specifically overcomes large bandwidth gap and frame structure difference. WULoc also proposes a periodical synchronization mechanism to synchronize UWB anchors with unstable local oscillators and extracts picosecond-level timestamps from Wi-Fi-UWB connection for TDoA calculation. Furthermore, WULoc estimates the Wi-Fi target's location using hyperbolic triangulation techniques.
- WULoc is implemented on USRP N310 (Wi-Fi target) and UWB DW1000 module (anchor), and evaluated under various scenarios, including an indoor lab (128 m^2), an indoor stadium (700 m^2), and an outdoor campus lawn (180000 m^2). The experimental results demonstrate that WULoc achieves a 5.3 meters average error at 240 meters distance in the outdoor scenario, achieving 242% range extension compared to state-of-the-art approaches. The results also show the robustness and effectiveness of WULoc under various indoor scenarios, including non-line-of-sight (NLoS) lab deployment and movement in the stadium.

2 MOTIVATION

2.1 The Limitation of Existing Wi-Fi Localization Systems

Existing techniques for Wi-Fi localization mainly rely on processing physical layer information, such as Received Signal Strength Indicator (RSSI) [18] and Channel State Information (CSI) [15, 24, 46, 48], extracted from transmissions between Wi-Fi targets and anchors. Since RSSI is affected by environmental factors like blockage and multipath interference, RSSI-based localization is typically suitable only for coarse applications, such as room-level positioning or zone tracking. To enhance precision, researchers have turned to CSI, which offers detailed insights into signal propagation, including time-of-flight (ToF), angle-of-arrival (AoA), and angle-of-departure (AoD). The accuracy of CSI-based methods depends on the number of antennas and available signal bandwidth, with recent Wi-Fi standards supporting up to eight antennas and 160 MHz bandwidth, allowing for improved localization precision. However, CSI is sensitive to SNR drops, particularly in long-range scenarios, leading to localization failures when SNR falls below a critical threshold. While many studies have focused on enhancing accuracy in confined areas, the localization range—crucial for real-world applications—has often been overlooked. To achieve long-range and precise localization, this paper introduces WULoc, which utilizes picosecond timestamp information from the Wi-Fi-UWB connection to accurately locate the Wi-Fi target at a distance of 240 meters. WULoc is inspired by two key opportunities.

2.2 Opportunity #1: UWB

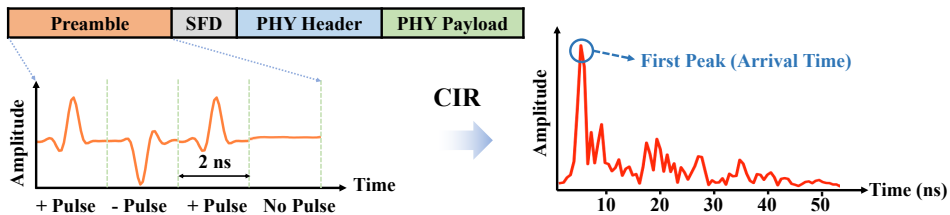


Fig. 1. Illustration of UWB PHY layer and CIR-based packet arrival time extraction.

Ultra-wideband (UWB) technology has gained significant popularity for its decimeter-level ranging accuracy, leading to its integration in smartphones like the iPhone (models 11 and later) and Samsung Galaxy 20 series, as well as in vehicles from manufacturers such as Volkswagen [35], BMW [5], and Hyundai [8]. This high precision is achieved through Channel Impulse Response (CIR) data, which allows for accurate estimation of the distance between UWB transmitters and receivers. Technically, a UWB PHY packet begins with a preamble field made up of sequences of positive and negative pulses or no pulse, as shown in Figure 1. This preamble is designed for perfect periodic autocorrelation, enabling the receiver to capture the CIR using a correlator [34]. The receiver then records the timestamp of the first path arrival time (the first peak in the CIR), allowing for precise distance measurement based on the UWB signal's preamble characteristics. To enhance ranging precision, UWB employs a high-speed oscillator, achieving picosecond-level (15.62 ps) timestamp resolution. Operating across a wide frequency band from 3.1 GHz to 10.6 GHz, UWB devices transmit at low power (typically around -14 dBm) to coexist with other wireless systems [39]. To receive these weak signals, UWB uses a simplified modulation scheme and a non-coherent receiver, ensuring robust reception over long distances. These two complementary capabilities—long-range low-SNR reception and high-precision timing—form the basis of the WULoc approach, enabling the integration of Wi-Fi and UWB for extended range and accurate localization. This integration is achieved through the proposed Wi-Fi-UWB connection establishment, inspired by the next opportunity—CTC.

2.3 Opportunity #2: Cross-Technology Communication

Wi-Fi-UWB connection establishment is inspired by cross-technology communication, which is proposed to establish the connection among IoT devices with incompatible physical layers. As the solution to bridge various wireless technologies, CTC has been widely investigated by academia and is increasingly attracting attention from the industry. For instance, Mitsubishi Electric Research Laboratories Inc. has developed a cross-technology neighbor discovery system to enable a Wi-Fi device to scan ambient ZigBee neighbors [20, 50]. A pilot study conducted by Ele.me, the largest food delivery company in China, and researchers at the University of Minnesota demonstrates the feasibility of building Wi-Fi to BLE CTC for creating BLE iBeacon service at Wi-Fi AP to track the couriers [31].

Technically, the existing CTC approaches are summarized into two categories: (i), wide-band to narrow-band CTC via **signal emulation** [26, 31, 50, 51]. Using Wi-Fi (20 MHz) to ZigBee (2 MHz) CTC as an example [26]: a Wi-Fi device emulates the target ZigBee signal by carefully customizing the payload of a Wi-Fi packet such that the corresponding transmitted Wi-Fi signal is recognized as a legitimate ZigBee packet at the commodity ZigBee devices. (ii), narrow-band to wide-band CTC via **symbol encoding** [45, 52]. In the Wi-Fi and ZigBee coexistence scenario, a ZigBee to Wi-Fi CTC is realized by customizing ZigBee symbols to generate special patterns at Wi-Fi physical layer. By recycling the patterns, the Wi-Fi device decodes the delivered CTC data. It is worth noting that this symbol encoding technique requires the wide-band receiver to be capable of extracting patterns from arbitrary received signals, even an incompatible signal. Although Wi-Fi to UWB communication ranges from narrow-band to wide-band, the technique of symbol encoding is not effective for establishing a Wi-Fi-UWB connection. This is because the low-cost UWB device is designed to process only UWB-compatible signals and cannot extract any patterns from incompatible Wi-Fi signals. Although signal emulation is typically used for wide-band to narrow-band CTC, WULoc introduces a range of innovative designs to facilitate communication from the Wi-Fi target to the UWB anchor. This Wi-Fi-UWB connection facilitates the estimation of TDoA and the location of the Wi-Fi target, as demonstrated in the following section.

3 WULOC OVERVIEW

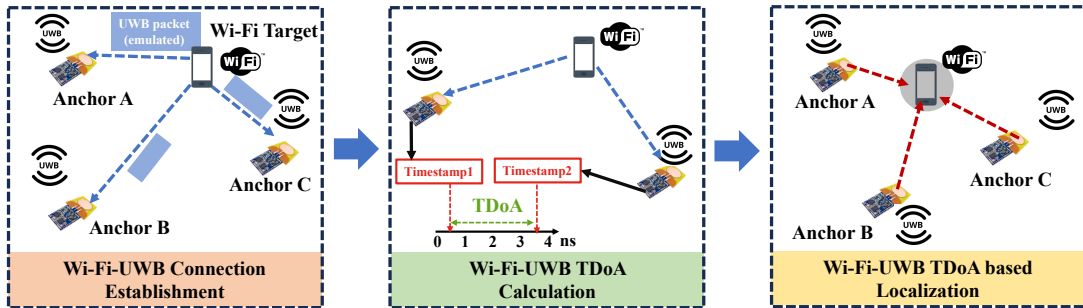


Fig. 2. WULoc comprises three steps: Wi-Fi-UWB Connection Establishment, Wi-Fi-UWB TDoA Calculation, and Wi-Fi-UWB TDoA based Localization.

As illustrated in Figure 2, the process of locating the Wi-Fi target using WULoc begins with the transmission of a specially customized Wi-Fi packet that emulates a UWB packet through the Wi-Fi-UWB Connection Establishment to UWB anchors. Upon receiving the emulated UWB packet, each anchor extracts the timestamp with a granularity of 15 ps, which is then used to calculate the Time Difference of Arrival (TDoA) between the two anchors in the Wi-Fi-UWB TDoA Calculation. Finally, hyperbolic triangulation is applied to estimate the

location of the Wi-Fi target in the Wi-Fi-UWB TDoA-based localization. It is worth mentioning that the three steps of WULoc present unique challenges, which are resolved by the detailed design as demonstrated next.

4 WULOC DESIGN

4.1 Wi-Fi-UWB Connection Establishment

To establish an efficient CTC from UWB to Wi-Fi, we need to utilize the high configurability of Wi-Fi devices to transmit specially designed payloads for simulating UWB signals. Existing physical layer CTC solutions can achieve communication from Wi-Fi to other narrower bandwidth protocols, but the bandwidth of UWB protocol is significantly higher than that of Wi-Fi. This gives rise to two issues: 1) precision loss due to CP (uncontrollable duration of 3.2 us exceeds the 0.999 us preamble unit duration). 2) The bandwidth gap.

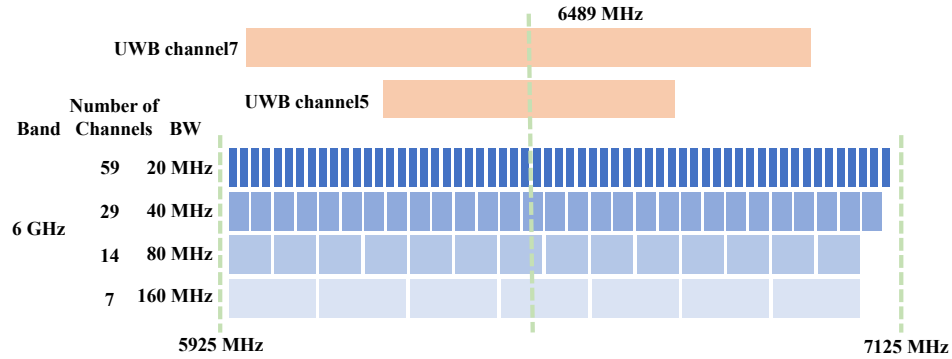


Fig. 3. The overlap frequency of UWB and Wi-Fi 6E.

4.1.1 Overcoming Frame Structure Difference. The frame structure differences between Wi-Fi and UWB introduce challenges for WULoc to establish communication from the Wi-Fi target to UWB anchors. As the basic transmission unit, the symbols, are significantly different – UWB uses a 0.996 us symbol [1], while Wi-Fi symbols last for multiples of 4 us [2]. Even worse, each Wi-Fi symbol contains a 0.8 to 3.2 us CP signal, which is automatically filled and poses additional uncertainty in generating UWB-compatible Wi-Fi packets. Our insights to overcome this challenge is that the Wi-Fi 802.11ax 6E standard offers various symbol configurations to control the Wi-Fi symbol duration and CP length, while the UWB standard supports multiple preamble sequence options. Specifically, we first choose an appropriate Wi-Fi duration to ensure that the Wi-Fi symbol duration is an integer multiple of the UWB symbol duration, thereby establishing a basic mapping between the symbols. To further enhance the accuracy of signal emulation, we select a specific UWB code index to make the CP as similar as possible to the original Wi-Fi signal, ensuring that the signal following the CP remains largely undistorted.

In order to maximize the precision of emulated UWB signals using Wi-Fi, we have chosen to utilize the IEEE 802.11ax standard adopted by Wi-Fi 6E. The IEEE 802.11ax standard, also known as Wi-Fi 6E, supports single-channel bandwidth modulation of up to 160 MHz. This enhanced bandwidth capability allows for more efficient transmission of data and enables us to better approximate the characteristics of UWB signals. As shown in Figure 3, the IEEE 802.11ax standard operates in the 6 GHz frequency band, which overlaps with the working frequency range of UWB devices. This frequency band compatibility between Wi-Fi and UWB makes our CTC design feasible. It allows for the possibility of establishing a communication link between Wi-Fi and UWB devices, enabling the transmission of information and facilitating cross-technology collaboration. By leveraging the features and capabilities of the IEEE 802.11ax standard, we can exploit the high configurability and adaptability of Wi-Fi devices to emulate UWB signals more accurately. This helps overcome the bandwidth limitations of Wi-Fi and enhances the potential for successful CTC communication between UWB and Wi-Fi technologies.

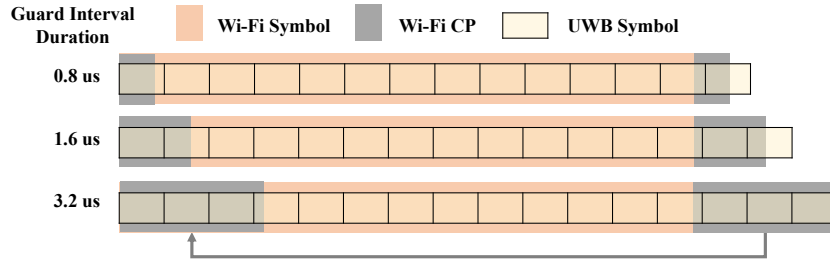


Fig. 4. Different duration of GI.

In the IEEE 802.11ax standard, the cyclic prefix (CP) plays a crucial role in mitigating inter-symbol interference caused by multipath propagation. It is employed in orthogonal frequency-division multiplexing (OFDM) modulation. The CP is a replicated portion of an OFDM symbol that is inserted before each symbol. It forms a cyclic structure by copying a portion of the symbol and appending it at the beginning. The length of the CP is typically a small fraction of the OFDM symbol length. By utilizing the CP, the IEEE 802.11ax standard effectively addresses interference in wireless channels caused by multipath propagation and frequency domain distortion. This enhances the system's resistance to interference and improves transmission reliability.

As shown in Figure 4, the CP in IEEE 802.11ax poses challenges when emulating UWB signals in Wi-Fi. Each symbol in a UWB signal has a duration of approximately 1 us (993.58 ns), while the guard interval (GI) options in the IEEE 802.11ax standard are 0.8 us, 1.6 us, and 3.2 us. None of these options can fully accommodate multiple UWB symbols, resulting in errors in the fractional part of the CP. This situation leads to segmentation of the original UWB symbols, thereby reducing the accuracy of signal emulation and potentially impacting system performance. Due to the incomplete match between the CP and the duration of the UWB signal, distortion and discontinuity may occur during the emulation process. However, considering the unavoidable nature of the guard interval, after analysis and experimentation, we have chosen a 3.2-us guard interval as the physical layer modulation parameter for emulating the signal. Compared to the other two guard interval lengths, a 3.2-us guard interval only affects a symbol by 20%, which is acceptable for UWB devices to tolerate. By carefully selecting the guard interval duration, we can improve signal emulation accuracy and ensure timestamps' accuracy.

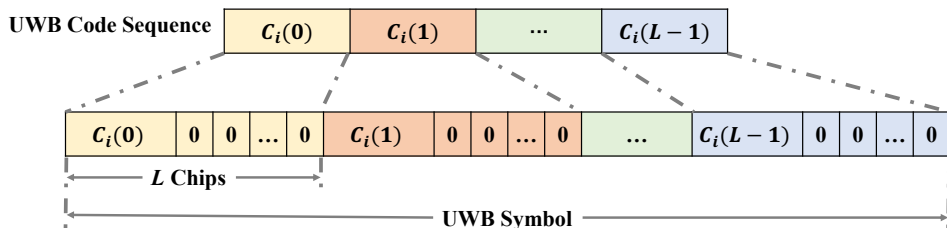


Fig. 5. Illustration of UWB Symbol structure.

As shown in Figure 5, a UWB preamble is a specific sequence of symbols or waveform that is transmitted at the beginning of a UWB transmission frame. It serves as a reference or synchronization signal to facilitate reliable communication and signal detection in UWB systems. The UWB preamble is designed to have known characteristics and patterns that can be easily recognized and processed by the receiving device. It helps establish timing synchronization, frequency synchronization, and other important parameters for the proper reception and decoding of the subsequent data symbols. The UWB preamble typically consists of a predefined sequence of UWB symbols with specific properties.

Table 1. UWB code index.

Code index	Code sequence
1	-0000+0-0+++0+-000+----00--0-00
2	0+0--0+0+000---0+-00+00++000
3	-+0++000-++-+00++0+00-0000-0+0-
4	0000+-00-00-++++0++000+0-0++0-
5	-0+-00++++000--0+++0-0+0000-00
6	++00+00-+-0++-000+0+0-+0+0000
7	+0000+-0+0+00+000+0++-0-+00-+
8	0+00-0-0++0000-+00-+0++-+0+00

UWB TX preamble code index is the index or identifier associated with a specific preamble code used in UWB transmission. In UWB systems, multiple preamble codes may be available or defined for different purposes, such as synchronization, channel estimation, or distinguishing different devices or channels. As shown in Table 1, each preamble code is uniquely identified by an index or code number. This index allows the receiving device to recognize and process the specific preamble code being used in the transmitted signal. By knowing the index, the receiver can correctly interpret and extract the information carried by the preamble code. The selection and assignment of preamble code indices are typically defined by the UWB system specifications or standards. The transmitter and receiver are designed to use the same set of predefined preamble codes, ensuring compatibility and successful communication.

To further reduce the error in Wi-Fi emulation, we selected a specific code index for operation. In the previous chapter, we chose a guard interval (GI) of 3.2 us. The Wi-Fi CP copies the last segment of the GI length to the beginning of the symbol, and this copied 3.2 us GI corresponds to an error segment of 0.2 us. A complete UWB symbol is 1 us long, including a 32-bit code sequence, and the 0.2 us segment corresponds to 7 bits. We calculated the correlation between the last 7 bits and the first 7 bits of each group of code sequences, considering the transmission channel. Ultimately, we chose to use code 4 to optimize our design.

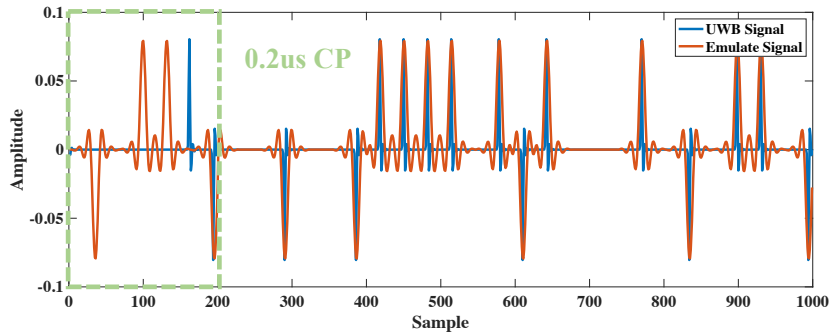


Fig. 6. Illustration of UWB signal and emulate signal.

As shown in Figure 6, we compare the emulated UWB preamble with the real UWB preamble and found that they are very similar but also have some differences. The signals before 0.2 us are almost completely different, which is due to the Wi-Fi CP. However, since this portion only accounts for a small fraction of the signal and not every symbol exhibits it, the resulting errors can be mitigated. On the other hand, the emulation preamble is smoother due to bandwidth limitations. Through our experiments, commercial UWB devices are able to successfully detect and demodulate the emulated preamble.

4.1.2 Overcoming Bandwidth Gap. The substantial bandwidth disparity presents a significant challenge, as Wi-Fi target devices are unable to generate a standard 500 MHz UWB signal waveform. Our technical contribution to addressing this gap involves leveraging the inherent design of low-cost UWB receivers by implementing a non-coherent detection approach, which relies on matching the demodulated symbol sequence in the preamble field for packet reception. This allows the non-coherent UWB receiver to receive a distorted signal as long as the demodulated preamble symbols match the expected preamble sequence. At a high level, our design to address the bandwidth issue is to enable the Wi-Fi target to emulate a special UWB signal—one that coincides with the Wi-Fi target’s operating channel. Although this overlapping section constitutes only a minor part of the conventional UWB signal, UWB anchors can still receive this specialized signal because of the non-coherent demodulation process used at UWB. The emulation of this specific signal is achieved using the signal emulation technique described in [26]. This is then integrated with the approach outlined in Section 4.1.1, which addresses differences in the frame structure, making a Wi-Fi-UWB connection feasible. A detailed analysis of how we bridge the bandwidth gap is presented below.

The physical layer of UWB technology exhibits robustness, enabling the successful reception of correct bit data even in the presence of signal distortion. The robustness of UWB physical layer can be attributed to its inherent characteristics and design. UWB signals employ wideband transmission techniques, distributing a large number of low-power pulses across the spectrum, which enhances their resistance to interference, multipath fading, and frequency-selective fading. Firstly, the wideband nature of UWB signals allows them to occupy multiple subcarriers in the spectrum, providing redundancy and diversity. Even if certain portions of the signal experience interference or distortion, other subcarriers can still provide effective information transmission. Secondly, UWB modulation schemes often utilize techniques such as differential modulation or phase modulation, which offer good noise and interference immunity. One commonly used modulation scheme for UWB preamble is the Binary Phase Shift Keying (BPSK):

$$s(t) = A * \text{con}(2\pi f_c t + \phi) \quad (1)$$

where $s(t)$ is the modulated UWB preamble signal as a function of time t , A is the amplitude of the carrier waveform, f_c is the carrier frequency, ϕ is the phase offset.

Additionally, UWB systems employ powerful signal processing algorithms and error correction techniques. The receiver employs forward error correction (FEC) codes to ensure the ability to detect and correct bit-level errors even in the presence of signal distortion.

In summary, the robustness of the UWB physical layer enables the successful reception of correct bit data even in the presence of signal distortion. The combination of the two strategies mentioned above ensures that commercial UWB devices can successfully demodulate and decode analog signals, as well as accurately record the correct timestamp, even in the presence of partial distortion in the Wi-Fi analog signal. It is also worth mentioning that our proposed Wi-Fi-UWB connection establishment is designed solely for signaling UWB anchors, not for transmitting data to UWB devices. In other words, triggering the UWB timestamp only requires the Wi-Fi target to reload and transmit the same customized Wi-Fi packet that has already been computed offline. Once the emulation is completed, the customized Wi-Fi packet can be reused for subsequent TDoA estimation and localization, without the need to execute the emulation process again. The ability to reuse the customized Wi-Fi packet for localization minimizes the overhead of implementing the Wi-Fi-UWB connection establishment. This makes the overall process more efficient and applicable to the widespread implementation on Wi-Fi devices.

4.2 Wi-Fi-UWB TDoA Calculation

As Wi-Fi-UWB Connection Establishment facilitates directional communication from the Wi-Fi target to UWB anchors, multiple UWB devices are employed as anchors to locate the Wi-Fi target by utilizing the high-precision timestamps provided by these anchors, allowing for the calculation of TDoA between each pair of UWB anchors.

However, as outlined in Section 2.2, the principle of UWB timestamp calculation indicates that the quality of the CIR affects timestamp extraction, meaning that timestamps derived from received emulated UWB packets can be influenced by emulation errors. Therefore, obtaining high-precision timestamps is both critical and challenging for TDoA estimation. This section explores how Wi-Fi channel bandwidth impacts the timestamps extracted at UWB anchors, followed by a detailed TDoA calculation that results in a hyperbola for localizing the Wi-Fi target.

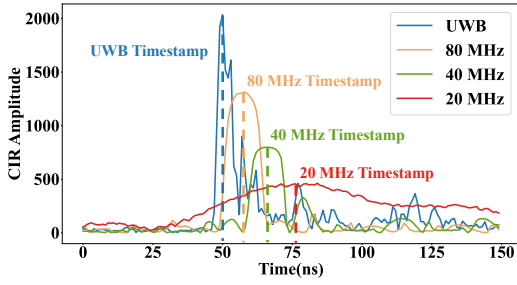


Fig. 7. CIR of UWB packets emulated by Wi-Fi with different bandwidth settings.

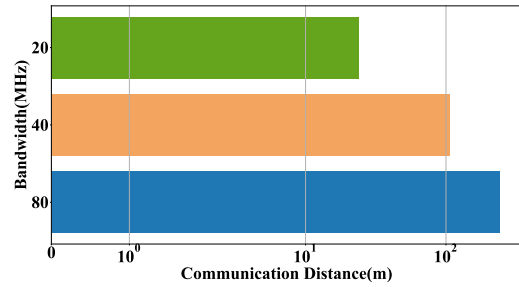


Fig. 8. Wi-Fi-UWB communication distance over the bandwidth settings of 20, 40, and 80 MHz.

Utilizing signal emulation design, WULoc achieves unidirectional cross-technology direct transmission from Wi-Fi devices to UWB devices. However, since the Wi-Fi device lacks the hardware capability to automatically record timestamps as present in UWB devices, traditional two-way ranging methods cannot be implemented. Therefore, we utilize a TDoA-based method to localize Wi-Fi targets by solely using one-way Wi-Fi broadcasts to multiple UWB anchors, without the need for UWB to transmit any signals to Wi-Fi. Additionally, we leverage the high power output of Wi-Fi devices to achieve long-range localization, while taking advantage of the high sampling rate of UWB to improve the accuracy of Wi-Fi target localization. In this approach, the Wi-Fi device broadcasts signals that are received by multiple UWB anchors. By measuring the time difference of arrival of the Wi-Fi signal at each anchor, we determine the distance between the Wi-Fi target and each anchor using the speed of signal propagation. By leveraging the high power output of Wi-Fi devices, the signals can propagate over longer distances, enabling long-range localization capabilities. Furthermore, the high sampling rate of UWB allows for precise measurements, enhancing the accuracy of Wi-Fi target localization. By combining the strengths of Wi-Fi and UWB, this approach enables efficient and accurate Wi-Fi target localization without the need for bidirectional communication between Wi-Fi and UWB devices.

The acquisition of TDoA is based on the timestamps from different anchors, which are automatically detected and recorded by UWB hardware. The timestamp is recorded when the first peak in the CIR is detected:

$$CIR(t) = \sum_{n=0}^{N-1} h(n) * \delta(t - \tau_n) \quad (2)$$

where $CIR(t)$ represents the Channel Impulse Response as a function of time t , $h(n)$ is the complex impulse response coefficient at discrete time index n , $\delta(t)$ is the Dirac delta function, τ_n is the delay associated with the n th path. The extraction of UWB timestamps relies on capturing the first peak of the CIR, which is influenced by the quality of the Wi-Fi bandwidth. As illustrated in Figure 7, the CIR with a 20 MHz bandwidth shows only a single broad peak, as all the finer peaks are merged due to the distortion caused by the 20 MHz bandwidth UWB packet emulation. Moreover, compared to the CIR extracted from a standard UWB packet, the peak of the 20 MHz bandwidth emulated UWB packet does not accurately represent the timing of packet arrival, resulting in an erroneous TDoA estimation. We also perform a preliminary experiment on the Wi-Fi-UWB communication

range across different bandwidths. As demonstrated in Figure 8, narrower bandwidths result in shorter reception ranges for the received emulated UWB packets due to considerable emulation distortion. As a result, bandwidth can impact both the accuracy of TDoA estimation and the range of the Wi-Fi-UWB connection, which may adversely affect WULoc's performance in terms of localization accuracy and range.

As shown in the Figure 2, target sends a emulating UWB packet, and anchor A and anchor B receive the emulating packet and record the detected packet time as timestamp. While, anchor A and anchor B, located at coordinates (x_A, y_A) and (x_B, y_B) , respectively. And the signal source of Wi-Fi target is located at an unknown position (x, y) . The time difference of arrival between the two receivers can be represented as:

$$TDoA_{AB} = \Delta t_{AB} = d_{AB}/c \quad (3)$$

where d_{AB} is the Euclidean distance between the target and anchor B minus the distance between the target and anchor A and c is the speed of signal propagation. Since the TDoA is a constant value for a given pair of receivers, it can be rewritten as:

$$c * \Delta t_{AB} = d_{AB} \quad (4)$$

The hyperbolic equation describes the possible positions (x, y) that satisfy the TDoA measurement:

$$\sqrt{(x - x_A)^2 + (y - y_A)^2} - \sqrt{(x - x_B)^2 + (y - y_B)^2} = c * \Delta t_{AB} \quad (5)$$

This equation represents a hyperbola in the positioning space. By having multiple pairs of receivers and their corresponding TDoA measurements, a system of hyperbolic equations can be formed. The intersection points of these hyperbolic curves represent the potential locations of the target.

4.3 Wi-Fi-UWB TDoA based Localization

TDoA hyperbolic localization is a method used to estimate the location of a signal source based on the time differences of arrival measured at multiple anchors. This method relies on the principle that the difference in arrival times at different anchors corresponds to hyperbolic curves in the positioning space.

WULoc needs to comprehensively calculate the unique positioning result by combining the TDoA data between multiple anchors. The two anchors can only determine two curves according to the hyperbolic equation, which cannot be used for localization. At least three anchors can locate the target position by finding the intersection point of the six curves.

In a hyperbolic equation, there are two curves associated with it. However, in reality, the target can only lie on one of these curves because the process of constructing the hyperbolic equation ignores the positive or negative values of the TDoA. The two hyperbolic equations may have multiple numerical solutions, but by introducing the constraint of the positive and negative values of TDoA, we effectively deal with the intersection of two curves instead of six curves. This significantly reduces the occurrence of erroneous localization results.

We obtain a set of all intersection $C_{m,n}(x, y)$ and assign different weights $w_{m,n}$ to different intersections, where m and n represent two different anchors corresponding to the current intersection. The target location that integrates multiple anchors can be obtained as:

$$T(x, y) = \frac{\sum_{m=1}^{K-1} \sum_{n=m}^K w_{m,n} \times C_{m,n}(x, y)}{\sum_{m=1}^{K-1} \sum_{n=m}^K w_{m,n}} \quad (6)$$

where $T(x, y)$ represents the localization of the target and K represents the number of anchors. In order to improve the accuracy of target localization in our model, we implemented a unique approach where we assigned different weights to different intersections instead of taking the average of several intersections. Our research revealed that the amplitude of CIR peak has a significant impact on the accuracy of angle estimation. To address this, we introduced an additional feature input A_{CIR} . By incorporating feature A_{CIR} , we were able to assign different weights to different anchors. Specifically, the weight $w_{m,n}$ of the intersections is obtained through a

combination of the two anchors, i.e $w_{m,n} = \log A_{CIR}(m) + \log A_{CIR}(n)$. Overall, TDoA hyperbolic localization utilizes the time difference of arrival measurements between multiple anchors to create a system of hyperbolic curves, allowing for the estimation of the target location by finding the intersection points of these curves.

5 UWB SYNCHRONIZATION

UWB devices rely on accurate timestamps to calculate TDoA for localization, hence a high-performance synchronization mechanism is necessary. In long-range positioning scenarios, it is challenging to connect multiple anchors using optical fibers, which would incur significant deployment costs. Therefore, WULoc employs a wireless broadcast synchronization mechanism to achieve synchronization among anchors. However, UWB nodes are low-cost devices, and there can be substantial crystal oscillator variance between different devices, especially with significant temperature effects. This necessitates the design of an efficient wireless synchronization mechanism. UWB is quite sensitive to temperature change, which is mainly caused by the internal warm up by transmission. Because low-cost in the hardware design, resulting in low-quality oscillator. This is different from UWB-UWB two-way ranging synchronization. The challenge of this module is to achieve synchronization with a unidirectional connection under extremely temperature-sensitive hardware.

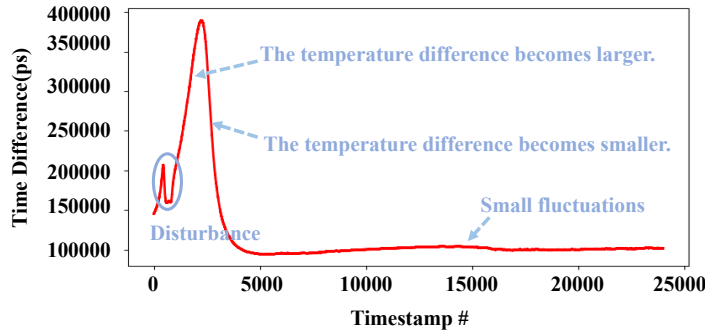


Fig. 9. Time difference caused by temperature fluctuation.

Commercial UWB devices utilize the DW1000 front-end chip, which is equipped with multiple timestamp registers for storing the timestamp information of transmitted and received data packets. These registers enable the reading and writing of timestamp values to support time measurement and localization applications. The receive timestamp register, in particular, has a length of 14 bits in decimal format. A value of 1 in the register represents a time of 15.620 picoseconds (ps), which theoretically corresponds to a very high precision in terms of the arrival time accuracy. This high precision allows the DW1000 to provide accurate measurements of transmission distances, $\Delta d = \Delta t * c = 15.62 * 10^{-12} * 3 * 10^8 = 4.7 * 10^{-3}(m)$.

However, as shown in Figure 9, UWB is quite sensitive to temperature changes, primarily caused by internal warming during transmission. This sensitivity is mainly due to cost-saving measures in hardware design, resulting in lower-quality oscillators. Each timestamp is generated by the local oscillator, which can introduce significant timestamp errors when calculating TDoA, thereby affecting localization accuracy. Traditional UWB systems mitigate this issue through Two Way Ranging (TWR) strategies, cleverly containing the errors within the chip itself and reducing the impact of oscillator variations between different chips, thus minimizing errors. In our design, we have implemented unidirectional communication from Wi-Fi to UWB, which renders the TWR strategy unsuitable. To address this, we have introduced an initiator and clock alignment mechanism. These mechanisms aim to minimize the impact of timestamp errors caused by temperature changes and oscillator variations, thereby improving the overall localization accuracy.

TDoA is a localization technique that determines the location of a signal source by measuring the time difference of arrival between different receivers. In practical applications, accurate TDoA values require synchronization among the receivers. The wireless synchronization mechanism ensures time synchronization among different devices by transmitting synchronization signals. The Initiator plays an important role in this process as it initiates communication and sends synchronization signals to other devices. When the receivers receive the synchronization signals, they synchronize their local clocks based on the timestamp of the signal. This enables all devices to perform TDoA calculations on the same time reference. Through the wireless synchronization mechanism and the role of the Initiator, TDoA calculation can eliminate time discrepancies between devices and provide accurate time difference of arrival values. This is crucial for localization and distance measurement applications as precise TDoA values are used to determine the position of signal sources and achieve high-precision localization and distance measurement.

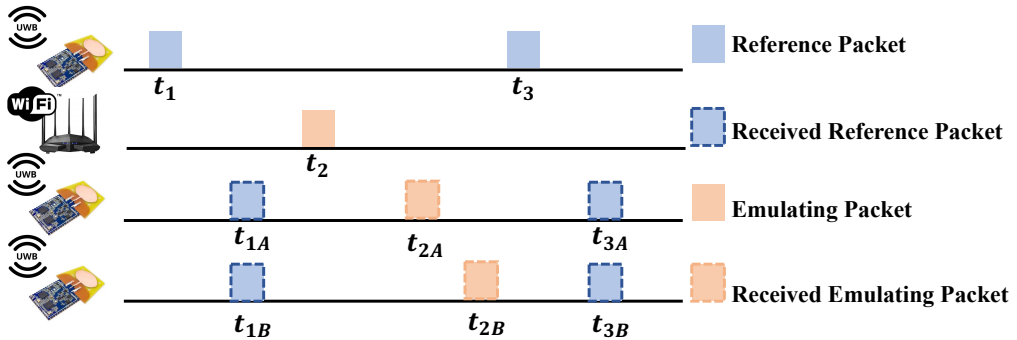


Fig. 10. WULoc timing diagram.

Initiator signal is denoted as t_{1A} and t_{1B} , respectively. Anchor A receives the target signal at time t_{2A} , while anchor B receives the target signal at time t_{1B} . Due to the local timestamps recorded by A and B, along with the influence of temperature, significant errors can occur. However, the two reference times sent by the Initiator are accurate. Therefore, we utilize these reference times to map the time at anchor B to anchor A, enabling us to calculate the TDoA accurately:

$$TDoA'_{AB} = (t_{2A} - t_{1A}) - \frac{t_{3A} - t_{1A}}{t_{3B} - t_{1B}} \times (t_{2B} - t_{1B}) \quad (7)$$

It is important to note that our proposed UWB synchronization design has a negligible impact on Wi-Fi traffic performance. This is because the UWB transmission power is typically -14.3dbm [39] for 500MHz, which is too weak to cause interference to Wi-Fi traffic. This is also validated by the study [6], demonstrating that UWB traffic has almost no measurable impact on Wi-Fi traffic when the UWB device is situated at least 0.7 meters away from the Wi-Fi device. Therefore, in our localization scenario, the UWB initiator is deployed at a much greater distance than 0.7 meters, which ensures that the WULoc system remains immune to any potential overhead introduced by the UWB synchronization process.

6 DISCUSSION

6.1 AoA-based Localization Technique vs WULoc

AoA based localization has been widely explored for Wi-Fi [24, 46, 48], UWB [62], and LoRa [27]. Technically, to calculate AoA, the wireless device should be equipped with multiple antennas, a feature commonly supported by Wi-Fi devices and some UWB devices, such as the DW 3x20 series radio chips [40]. In contrast, the WULoc

system relies solely on timestamp information, independent of the number of antennas. This allows WULoc to function alongside AoA-based techniques, creating the potential for integrating these techniques with WULoc to enhance localization performance. WULoc relies on TDoA and hyperbola triangulation, requiring at least three anchors to create a minimum of two hyperbolas. By incorporating AoA-capable UWB devices into the WULoc system, the number of anchors needed can be reduced. For example, with two AoA-capable UWB anchors, each can provide an AoA estimation, allowing the target to be located within a candidate area based on multiple rounds of AoA estimation and associated errors. Subsequently, TDoA data from WULoc can further refine this candidate area for more precise target localization.

6.2 Impact of Channel Allocation on WULoc

The distinct channel allocation mechanisms employed by UWB and Wi-Fi lead to various center frequency misalignments or offsets. For instance, the center frequency of Wi-Fi channel 87 exhibits a 104.6 MHz offset from that of UWB channel 5, while Wi-Fi channel 103 and UWB channel 5 have a 24.6 MHz center frequency offset. Interestingly, the WULoc system demonstrates natural immunity to these center frequency offsets. This is attributed to the BPSK demodulation employed in the UWB system, which relies solely on the phase comparison between pulses, and the UWB receiver's PHY layer. When a UWB signal is received, the UWB receiver automatically compensates for sampling offsets and other jitters to synchronize the phase with the receiver's clock for accurate demodulation. As a result, even with a center frequency offset, a partially overlapping Wi-Fi signal can still emulate a UWB packet, since the received signal is adjusted to ensure that the distorted signal maintains the same phase for both bit 0 and bit 1. To validate this, we conduct an experiment to demonstrate the robustness of the WULoc system against center frequency offset in Section 7.5. Additionally, it is worth noting that the 5.925 GHz - 7.125 GHz frequency band [54], utilized by the WULoc system, is openly available in the Americas, including the United States, Canada, Brazil, and some Asian countries, such as Saudi Arabia, and South Korea. This accessibility of the designated spectrum enhances the potential for the widespread deployment and adoption of WULoc system.

6.3 Impact of the Distance Between UWB Anchors

The distance between UWB anchors affects the localization range and precision. According to the principle of triangulation [16], the maximum range of TDoA estimation is limited to the distance between the two anchors, as the difference between the lengths of any two sides of a triangle is always less than that of the third side. In other words, when accounting for TDoA estimation errors, if the estimation error surpasses the distance between the anchors, the WULoc localization becomes unavailable. To analyze this phenomenon, the relationship among the distance between UWB anchors, Wi-Fi bandwidth, and is formulated in the following equation:

$$D_{AB} \geq \epsilon(D_A, D_B, BW) \quad (8)$$

where, ϵ represents the TDoA estimation error that is determined by the distance between the target Wi-Fi device and each anchor, and BW is the bandwidth of the Wi-Fi target. Therefore, to apply WULoc to a wider range - supporting a longer D_A and D_B -the distance between anchors should be increased. Fortunately, as Section 7.2.2. shows, WULoc achieves a TDoA estimation error of less than 1.5 m within a localization range of 240 m, significantly less than the 10 m distance between anchors, making WULoc suitable for long-range localization. Additionally, the distance between the anchors impacts the curvature of the hyperbolas; if they are placed too close, the hyperbolas become increasingly distorted. As a result, the intersections of these highly distorted hyperbolas lead to larger errors, reducing the precision of WULoc, as demonstrated in Section 7.2.2.

7 EVALUATION

7.1 Implementation



Fig. 11. Evaluation testbed.

As shown in Figure 11(a) and Figure 11(b), the devices utilized in the experiment include a transmitting device, a few receiving devices, and an initiator device. We select DW 1000 module as UWB anchors and initiators because Qorvo's DW series UWB modules are commonly used in various commodity devices, such as Google Pixel 6 smartphone. Not only that, but many smartphones have already been deployed with Qorvo's UWB chips, such as the Google Pixel 8, Google Pixel 9, NIO Phone 2, and Samsung Galaxy S24 [53]. By utilizing only the timestamps provided by the DW1000, WULoc can be effectively deployed in commodity UWB devices. The Wi-Fi target is implemented on USRP N310, compliant with the Wi-Fi 802.11ax standard and supported by the Matlab WLAN toolbox.

The USRP N310 serves as the transmitter, responsible for generating and transmitting the 125 MHz Wi-Fi signal periodically with a transmission period of 60 ms. To operate the USRP N310, it is controlled and configured using the gnuradio software running on the connected host computer. The device also requires a stable power supply to ensure proper functionality during the experiment. The receiver is a UWB device that contains a commercial DW1000 chip. It operates on channel 2 and captures timestamp information from the received signals. The captured timestamp information is stored on a PC for further processing and analysis. The receiver is a UWB device equipped with a commercial DW1000 chip. It operates on channel 2 and is capable of capturing timestamp information from the received signals. To control the UWB device, we load python code to communicate with the device through the serial port. This allows for direct control and configuration of the device's parameters and functionalities. The UWB device is connected to the host computer using a USB data cable, which not only provides power to the device but also facilitates the transfer of data between the device and the host computer. The host computer receives the captured analog Wi-Fi signals from the UWB device and stores them for further processing and analysis. The stored data can be processed using appropriate algorithms and techniques to achieve localization or other desired objectives. The initiator device is another commercial UWB transmitter. It has a transmission period of 50 ms and is used to provide wireless synchronization services. The initiator device sends synchronization signals to facilitate wireless synchronization among different UWB devices.

We use a Bosch NP02 laser rangefinder, which has a maximum measurement range of 600 m and an accuracy of up to 0.5 m, to measure the ground truth TDoA and locations. TDoA is calculated from the measured distance

between the target and the anchors. To determine the ground truth location, we employ the rangefinder to measure the target's coordinates in each scenario. In the mobile scenario, we establish multiple checkpoints along the movement trajectory and measure each checkpoint statically before conducting the experiment. We then use WULoc to determine the moving location when the target steps on these checkpoints.

With this setup, the signal sent by the transmitter is a Wi-Fi signal that has been specially designed to emulate a standard UWB signal. This signal can be demodulated simultaneously by both Wi-Fi devices and UWB devices. The receiving device and the Initiator device, on the other hand, are standard commercial UWB devices. To evaluate the performance of our system, WULoc, we deploy different sets of transmitting and receiving devices in various indoor and outdoor scenarios. This allows us to test the TDoA error and positioning error of WULoc. By conducting these tests, we aim to assess the accuracy and effectiveness of our system in different environments.

7.2 Overall Performance of WULoc

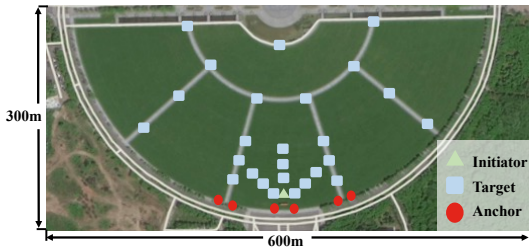


Fig. 12. Outdoor scenario: 300*600 m² campus lawn.

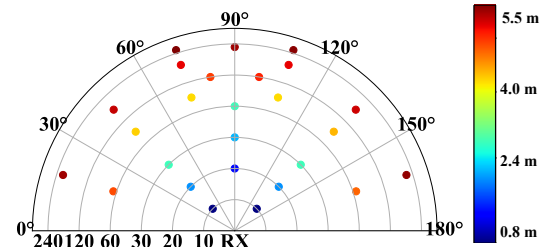
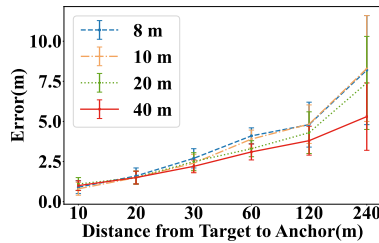
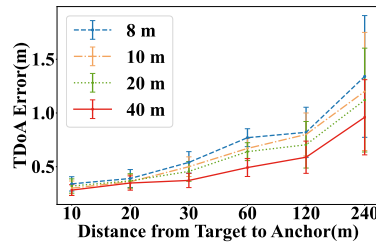


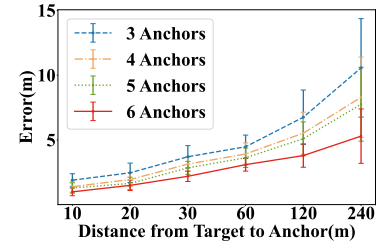
Fig. 13. Localization error in campus lawn.



(a) Localization error over Wi-Fi target to UWB anchor distances, with respect to different anchor-to-anchor distance.



(b) TDoA error over Wi-Fi target to UWB anchor distances, with respect to different anchor-to-anchor distance.



(c) Localization error over Wi-Fi target to UWB anchor distances, with respect to different number of anchors.

Fig. 14. WULoc performance in large campus lawn.

7.2.1 WULoc in Campus Lawn. As shown in Figure 12, we evaluate WULoc on a 300 × 600 m² campus lawn, including 26 target locations ranging from 10 m to 240 m. In Figure 13, the points indicate target positions. The deep blue point at 10 m shows the minimum localization error of 0.8 m, while the deep red point at 240 m indicates the maximum error of 5.5 m. These results also highlight the relationship between the target's angle and the anchor. For example, at a distance of 20 m, the error at 45° is 1.8 m, whereas at 90°, it is 1.2 m. Similarly, at 30 m, the errors are 1.8 m at 45° and 1.2 m at 90°.

7.2.2 Impact of Distance Between Anchors. We evaluate WULoc's performance on the outdoor lawn across various distances, focusing on localization error and TDoA error with respect to different distances between anchors. As shown in Figure 14(a) and Figure 14(b), localization and TDoA error decreases as the distance between

anchors increases. Comparing different anchor distances reveals that greater separation improves localization accuracy, as larger distances yield finer more precise TDoA hyperbolas. For example, at 240 m, when the anchor distance is 40 m, the localization error is 5.3 m, but reducing the anchor distance to 8 m increases the error by 58%, to 8.2 m.

7.2.3 Impact of Number of Anchors. As shown in Figure 14(c), we also evaluate the impact of the number of anchors on WULoc performance. Across all target-to-anchor distances, using more anchors for localization consistently yields better results than using fewer anchors. At 10 m, the localization error with six anchors is 0.97 m, compared to 1.9 m with three anchors. At a distance of 240 m, the localization errors are 5.3 m with six anchors and 10.3 m with three anchors, representing a 94% increase.

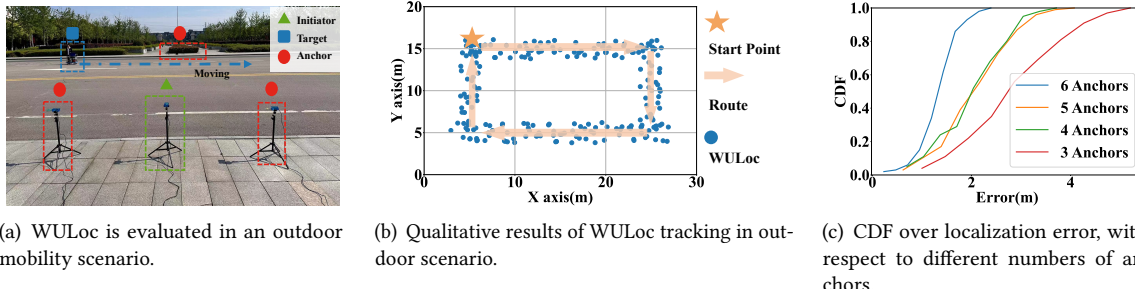


Fig. 15. WULoc performance under mobility in outdoor scenario.

7.2.4 Outdoor Mobility. We place the Wi-Fi target device on a trolley and evaluate the WULoc performance under mobility at the speed of 0.5 m/s in both outdoor and indoor scenarios. We predefine 100 checkpoints evenly distributed along the trajectory and the ground-truth location is obtained as explained in Section 7.1. As shown in Figure 15(a), we push the trolley on a flat outdoor area, forming a complete rectangular trajectory. The results, shown in Figure 15(b), indicate that the localization results closely follow the ground-truth trajectory, with a maximum error of around 2.1 m when six anchors are employed. Figure 15(c) demonstrates that the number of anchors significantly affects the localization of moving targets; using three anchors results in a maximum error of up to 5 m. This increased error is due to greater signal fluctuations encountered when the target is in motion compared to static scenarios.

7.3 WULoc in Indoor LoS and NLoS Scenarios

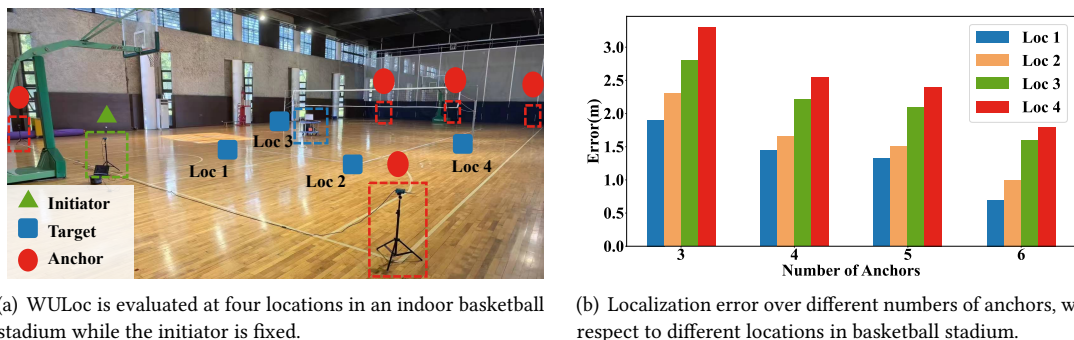


Fig. 16. WULoc performance in an indoor basketball stadium.

7.3.1 Basketball Scenario (Indoor LoS). Static Evaluation in Basketball Stadium. We evaluate the indoor performance of WULoc in a basketball stadium. As shown in Figure 16(a), the basketball stadium measures $20 \times 35 \text{ m}^2$. Figure 16(b) illustrates the localization error of WULoc in the indoor open-space scenario, with Loc 1-4 representing four different locations within the stadium, arranged by increasing distance from the anchors. The results indicate that localization error increases with distance from the anchors; for instance, Loc 1, approximately 5 m from the anchor, has an error of 0.72 m, while Loc 4, about 18 m away, has an error of approximately 1.77 m. Additionally, using more anchors improves localization performance. With six anchors, WULoc achieves a localization error of 0.72 m, whereas using only the three closest anchors to Loc 1 results in an error that is 152% greater, at 1.72 m.

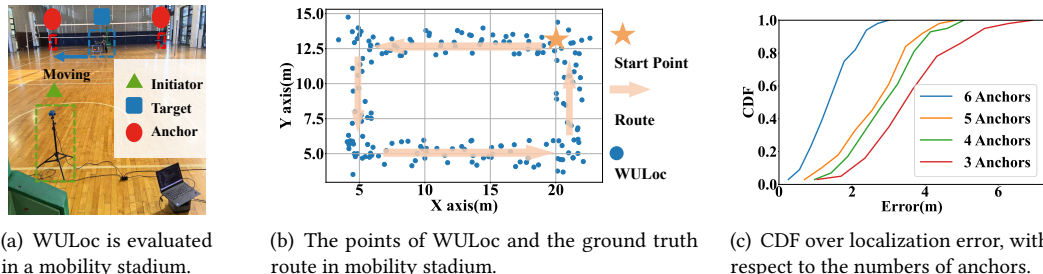


Fig. 17. WULoc performance under mobility in indoor scenario.

Mobility Evaluation in Basketball Stadium. In the scenario shown in Figure 17(a), we evaluate WULoc for indoor mobility. Figure 17(b) demonstrates that WULoc effectively tracks the moving target indoors. The maximum error in the indoor scenario is 2.6 m, which is slightly higher than in the outdoor scenario, with a more significant increase in error during turns. As shown in Figure 17(c), WULoc's performance using three anchors is poorer, with the maximum estimated error reaching 7 m because the complex indoor reflection contributes to increased localization errors, while using multiple anchors for joint tracking is able to mitigate this issue.

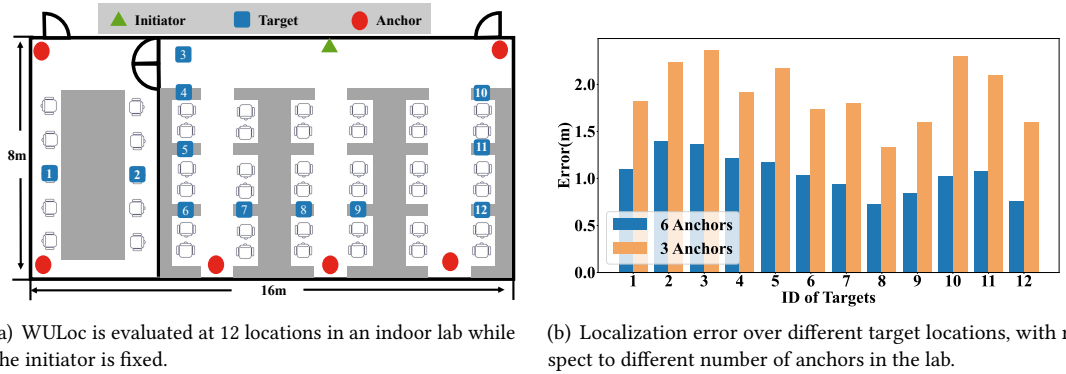


Fig. 18. WULoc performance in an indoor lab.

7.3.2 Lab Scenario (Indoor NLoS). We also evaluate the performance of WULoc in an indoor lab of $8 \times 16 \text{ m}^2$. As shown in Figure 18(a), compared to the basketball stadium, the interior of the lab is more crowded, with multiple desks and office chairs placed around. Additionally, it has a separate meeting room (location 1 and 2) that is partitioned by a glass wall. Figure 18 shows the experimental results. It proves that the crowded indoor environment leads to a decline in the performance of WULoc. Even with the utilization of 6 anchors for

localization, the maximum localization error is 1.41 m. With 3 anchors, the maximum indoor localization error is 2.37 m, while with 6 anchors, the maximum indoor localization error is 1.41 m, which occurred at the target locations of ID 3 and ID 2, respectively. This is because the target at the ID 3 location is separated from 2 of the nearest anchors by a glass door, which affects the localization performance.

7.4 Comparison with SoTA

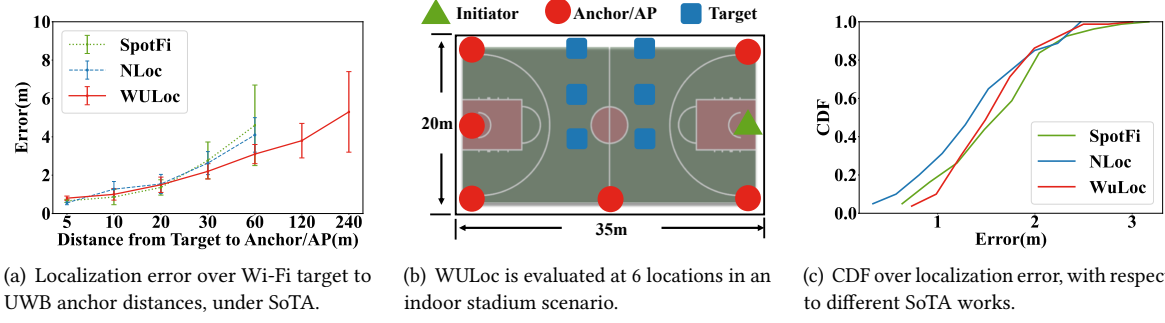


Fig. 19. Comparison with SoTA.

We compare WULoc with two SoTA design, including SpotFi [24], and NLoc [61]. the communication range limitation of Wi-Fi makes two state-of-the-art designs ineffective when the distance exceeds 100 meters, primarily due to their sensitivity to drops in SNR, as explained in Section 2.1. In contrast, WULoc is primarily based on the low-SNR reception capabilities of UWB, allowing it to achieve long-range localization. The results show that at a distance of 5 m, WULoc’s localization accuracy is 0.79 m, slightly lower than NLoc’s 0.56 m. This is because Wi-Fi uses CSI to calculate AoA for positioning, and in short-range scenarios without obstructions, AoA-based methods perform slightly better than WULoc. As the communication distance increases, NLoc and SpotFi become ineffective beyond 80 m. We also compare our WULoc with other state-of-the-art methods in an indoor scenario. In Figure 19(b), the red dots represent the positions of anchors or Wi-Fi APs, while the blue squares indicate the Wi-Fi targets scattered around the center of the anchors or APs. The evaluation results are presented in Figure 19(c). While NLoc demonstrates the best performance, with 90% of localization errors below 2.1 m, WULoc also performs well, with 90% of localization errors below 2.5 m.

7.5 Impact of WiFi Bandwidth and Channel Allocation

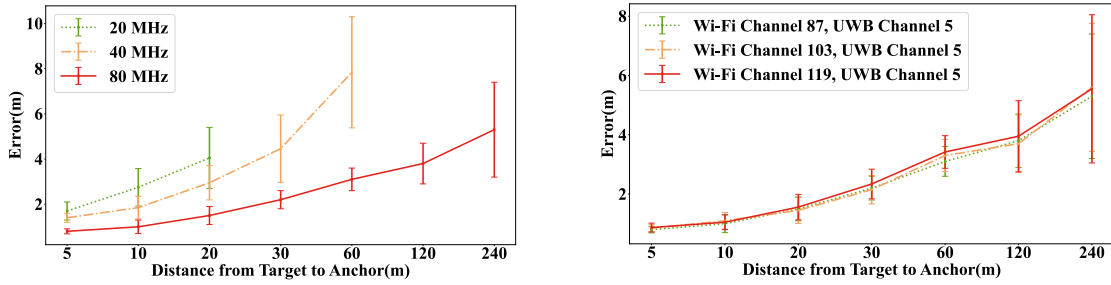


Fig. 20. WULoc localization error under different Wi-Fi bandwidth.

Fig. 21. WULoc localization error under different Wi-Fi and UWB channel settings.

As shown in Figure 20, we evaluate the localization error of WULoc with different bandwidths at different distances. Due to the range limitation of 20 MHz Wi-Fi signals, the distance between anchors is fixed at 10m when testing the 20 MHz signal. The experimental results show that the wider the Wi-Fi bandwidth, the smaller the localization error. When the bandwidth is 20 MHz, the localization error at a distance of 20 m is 4.1 m, while the error with 80 MHz bandwidth is 1.5 m. When the bandwidth is 40 MHz, the localization error at a distance of 60 m is 7.8 m, while the error with 80 MHz bandwidth is 3.1 m.

To evaluate the impact of the channel allocation, we conduct an experiment to show WULoc performance using overlapping channels: UWB channel 5 (6489.6 MHz) and Wi-Fi channels 87 (6385 MHz), 103 (6465 MHz), and 119 (6545 MHz), with their corresponding channel offsets of 104.6 MHz, 24.6 MHz, and -55.4 MHz. However, since the USRP N310 cannot operate at frequencies above 6 GHz, we configured the UWB anchors to use channel 3 (4492.8 MHz) and set the Wi-Fi channels on the USRP N310 to center frequencies of 4388.2 MHz, 4468.2 MHz, and 4548.2 MHz, respectively, to maintain the same center frequency offsets. The results shown in Figure 21 indicate that the center frequency offset of different Wi-Fi and UWB channels has almost no impact on localization performance.

8 RELATED WORK

8.1 RF-based Localization and Sensing

Table 2. Comparison of RF-based localization technologies.

Ref.	Technology	# of antennas per AP	Approach	PHY Info.	Tested area (m^2)
SpotFi [24]	Wi-Fi	≥ 3	AoA+ToF	CSI	160
SiFi [15]	Wi-Fi	≥ 1	ToA	CSI	4620
NLoc [61]	Wi-Fi	≥ 3	ToF	CSI	610
TM [57]	Wi-Fi	≥ 1	IMU+RSSI	RSSI	22400
DAFI [25]	Wi-Fi	≥ 3	Fingerprint	CSI	12
Wepos [18]	Wi-Fi	≥ 1	Fingerprint	RSSI	Mall
TagFi [46]	Wi-Fi	≥ 3	AoA+AoD	CSI	372
ClickLoc [55]	Wi-Fi	≥ 1	CV+Fingerprint	Fingerprint	Mall
WiPolar [48]	Wi-Fi	≥ 5	AOA	CSI	15
ILLoc [19]	LoRa	≥ 1	TDoA	Timestamp	7700
OWLL [4]	LoRa	≥ 1	TDoA	Phase	66000
Seirios [27]	LoRa	≥ 2	AoA	CSI	6000
ITrack [7]	UWB	≥ 1	IMU+TDoA	CIR	4.08
ULoc [62]	UWB	≥ 4	AoA	FPI+CIR	59.5
UWB ² [63]	UWB	≥ 1	ToF	Timestamp	25
VULoc [56]	UWB	≥ 1	TWR	Timestamp+CIR	7200
Surepoint [23]	UWB	≥ 3	TWR	Timestamp	144
SALMA [17]	UWB	≥ 4	TWR	Timestamp+CIR	48

As shown in Table 2, we summarize and compare the localization technologies of Wi-Fi [28, 29, 42, 43], LoRa [14], and UWB [9], and distinguish them by different aspects. Researchers propose various Wi-Fi localization systems based on different methods, including AoA, ToF, and RSSI etc., SpotFi [24] is the first method that utilizes CSI to construct a new matrix for joint estimation of AoA and ToF on commodity Wi-Fi devices. SiFi [15] proposes a single AP-based indoor localization system, achieving sub-meter accuracy localization in a large area. NLoc [61] focuses on signal emission characteristics to improve the localization accuracy in NLOS scenarios. TM [57]

combines IMU information to enhance localization accuracy, while ClickLoc [55] integrates computer vision techniques for localization. DAFI [25] and Wepos [18] utilize fingerprint-based machine-learning models for indoor localization. TagFi [46] utilizes Wi-Fi signals to stimulate RFID tags, enabling the localization of RFID tags. WiPolar [48] proposes to leverage signal polarization from modern Wi-Fi devices for accurate multi-person tracking. Moreover, Wi-Fi has been widely applied in various sensing scenarios [11, 37, 47, 58–60].

For long-range localization, researchers have also proposed LoRa-based approaches. ILLoc [19] utilizes the phase information of the received LoRa signal to obtain TDoA for LoRa localization. OWLL [4] utilizes the TDoA method and aggregates multiple channels to enable LoRa node localization over a $7000m^2$ area. Seirios [27] employs MUSIC algorithm and spatial smoothing technique for long-range LoRa localization. For UWB localization, some works introduce additional hardware, such as IMU [7], multiple antennas [62] and backscatter tags [63] to enhance localization performance. VULoc [56], Surepoint [23], and SALMA [17] leverage the TWR technique specified in UWB standard, coupled with CIR information and multi-antenna technology, to achieve real-time 3D localization. In addition, UWB devices are applied for sensing systems [3, 12, 32, 33, 36].

8.2 Cross-technology Communication

Table 3. Comparison of CTC technologies.

Ref.	Throughput	Direction	CTC layer	Bandwidth	Approach
WEBee [26]	High	Wi-Fi->ZigBee	PHY	Wide->Narrow	Emulation
SymBee [52]	Medium	ZigBee->Wi-Fi	Symbol	Narrow->Wide	Symbol encoding
ZiFi [38]	Low	ZigBee->Wi-Fi	Packet	Narrow->Wide	RSSI
BlueFi [10]	High	Wi-Fi->Bluetooth	PHY	Wide->Narrow	Emulation
WiBeacon [31]	High	Wi-Fi->Bluetooth	PHY	Wide->Narrow	Emulation
LTE2B [30]	High	LTE-U->ZigBee	PHY	Wide->Narrow	Emulation
TCTC [22]	Low	Wi-Fi->ZigBee	Packet	Wide->Narrow	Packet interval
X-MIMO [51]	High	Wi-Fi->ZigBee	PHY	Wide->Narrow	Emulation

As shown in Table 3, we research and compare different CTC works, which enable direct communication across different wireless technologies [14, 49]. WEBee [26] is the first to propose the signal emulation approach, directly emulating ZigBee signal at commodity Wi-Fi. SymBee [52] employs a symbol encoding approach to enable the CTC from narrow-bandwidth to wide-bandwidth technology. ZiFi [38] utilizes packet-level RSSI to realize CTC. BlueFi [10], WiBeacon [31] and LTE2B [30] respectively realize CTC among WiFi, Bluetooth, and LTE-U. X-MIMO [51] leverages emulation techniques and multi-antenna processing capabilities to bring multi-user MIMO into CTC.

9 CONCLUSION

This paper presents WULoc, a long-range and high-precision localization system that utilizes UWB devices to locate the target Wi-Fi device. WULoc achieves this by utilizing the picosecond timestamp capability of UWB anchors to calculate the TDoA, which is then used to estimate the location of the Wi-Fi target. WULoc specifically addresses several technical hurdles, including establishing the connection from the Wi-Fi target to UWB anchors despite the incompatibility between UWB and Wi-Fi physical layers, and synchronizing UWB anchors wirelessly given the significant clock drifts in the low-cost UWB anchors. Additionally, WULoc is resilient to Wi-Fi-UWB channel offsets that arise from channel allocation. The performance of WULoc is evaluated across various scenarios, including a $300\times600 m^2$ campus lawn, a $20\times25 m^2$ indoor basket stadium and an indoor lab, under line-of-sight (LoS), non-line-of-sight (NLoS), and mobility conditions. The experiments demonstrate that

WULoc achieves an average error of 5.3 meters when the target is 240 meters away from the anchors, a level of range and accuracy that existing Wi-Fi-to-Wi-Fi baseline methods cannot provide. Since WULoc relies solely on timestamp information, it can be integrated with other localization systems that utilize channel information or multi-antenna features to enhance localization results. With these advantages, WULoc is expected to be widely adopted as a complementary solution to GPS in long-range localization applications.

ACKNOWLEDGMENTS

We thank all the reviewers for their insightful feedback to improve this paper. This work is partially supported by the National Natural Science Foundation of China (Grants No. 62102332, 62272098, and U24B20152), Central University Basic Research Fund of China (Grants No. 2242024K40019), and the Natural Science Foundation of Jiangsu Province (Grants No. BK20241274).

REFERENCES

- [1] 2020. IEEE Standard for Low-Rate Wireless Networks. *IEEE Std 802.15.4-2020 (Revision of IEEE Std 802.15.4-2015)* (2020), 1–800. <https://doi.org/10.1109/IEEEESTD.2020.9144691>
- [2] 2021. IEEE Standard for Information Technology—Telecommunications and Information Exchange between Systems Local and Metropolitan Area Networks—Specific Requirements Part 11: Wireless LAN Medium Access Control (MAC) and Physical Layer (PHY). *IEEE Std 802.11-2020 (Revision of IEEE Std 802.11-2016)* (2021), 1–3534.
- [3] Boyd Anderson, Mingqian Shi, Vincent YF Tan, and Ye Wang. 2019. Mobile gait analysis using foot-mounted UWB sensors. *Proceedings of the ACM on Interactive, Mobile, Wearable and Ubiquitous Technologies* 3, 3 (2019), 1–22.
- [4] Atul Bansal, Akshay Gadre, Vaibhav Singh, Anthony Rowe, Bob Iannucci, and Swarun Kumar. 2021. OwlL: Accurate lora localization using the tv whitespaces. In *Proceedings of the 20th International Conference on Information Processing in Sensor Networks (co-located with CPS-IoT Week 2021)*. 148–162.
- [5] BMW. 2021. Introducing the BMW Digital Key Plus, <https://www.bmw.com/en/innovation/bmw-digital-key-plus-ultra-wideband.html>.
- [6] Hannah Brunner, Michael Stocker, Maximilian Schuh, Markus Schüßl, Carlo Alberto Boano, and Kay Römer. 2022. Understanding and mitigating the impact of Wi-Fi 6E interference on ultra-wideband communications and ranging. In *2022 21st ACM/IEEE International Conference on Information Processing in Sensor Networks (IPSN)*. IEEE, 92–104.
- [7] Yifeng Cao, Ashutosh Dhekne, and Mostafa Ammar. 2021. ITrackU: tracking a pen-like instrument via UWB-IMU fusion. In *Proceedings of the 19th Annual International Conference on Mobile Systems, Applications, and Services*. 453–466.
- [8] Lim Chang-won. 2022. Hyundai auto group provides new digital key service for Samsung and Apple smartphones, <https://www.ajudaily.com/view/20220412113249182>.
- [9] Weiyan Chen, Fusang Zhang, Tao Gu, Kexing Zhou, Zixuan Huo, and Daqing Zhang. 2021. Constructing floor plan through smoke using ultra wideband radar. *Proceedings of the ACM on Interactive, Mobile, Wearable and Ubiquitous Technologies* 5, 4 (2021), 1–29.
- [10] Hsun-Wei Cho and Kang G Shin. 2021. BlueFi: bluetooth over WiFi. In *Proceedings of the 2021 ACM SIGCOMM 2021 Conference*. 475–487.
- [11] Han Ding, Jinsong Han, Chen Qian, Fu Xiao, Ge Wang, Nan Yang, Wei Xi, and Jian Xiao. 2018. Trio: Utilizing tag interference for refined localization of passive RFID. In *IEEE INFOCOM 2018-IEEE Conference on Computer Communications*. IEEE, 828–836.
- [12] Rong Ding, Haiming Jin, Dong Xiang, Xiaocheng Wang, Yongkui Zhang, Dingman Shen, Lu Su, Wentian Hao, Mingyuan Tao, Xinbing Wang, et al. 2023. Soil Moisture Sensing with UAV-Mounted IR-UWB Radar and Deep Learning. *Proceedings of the ACM on Interactive, Mobile, Wearable and Ubiquitous Technologies* 7, 1 (2023), 1–25.
- [13] Iman ElKassabi and Atef Abdrabou. 2022. An experimental comparative performance study of different WiFi standards for smart cities outdoor environments. In *2022 IEEE 13th Annual Ubiquitous Computing, Electronics & Mobile Communication Conference (UEMCON)*. IEEE, 0450–0455.
- [14] Demin Gao, Haoyu Wang, Shuai Wang, Weizheng Wang, Zhimeng Yin, Shahid Mumtaz, Xingwang Li, Valerio Frascola, and Arumugam Nallanathan. 2024. Wilo: Long-range cross-technology communication from wi-fi to lora. *IEEE Transactions on Communications* (2024).
- [15] Wei Gong and Jiangchuan Liu. 2018. SiFi: Pushing the limit of time-based WiFi localization using a single commodity access point. *Proceedings of the ACM on Interactive, Mobile, Wearable and Ubiquitous Technologies* 2, 1 (2018), 1–21.
- [16] Paolo Grasso, Mauro S Innocente, Jun Jet Tai, Olivier Haas, and Arash M Dizqah. 2022. Analysis and accuracy improvement of uwb-tdoa-based indoor positioning system. *Sensors* 22, 23 (2022), 9136.
- [17] Bernhard Großwindhager, Michael Rath, Josef Kulmer, Mustafa S Bakr, Carlo Alberto Boano, Klaus Witrisal, and Kay Römer. 2018. SALMA: UWB-based single-anchor localization system using multipath assistance. In *Proceedings of the 16th ACM Conference on Embedded Networked Sensor Systems*. 132–144.

- [18] Baoshen Guo, Weijian Zuo, Shuai Wang, Wenjun Lyu, Zhiqing Hong, Yi Ding, Tian He, and Desheng Zhang. 2022. Wepos: Weak-supervised indoor positioning with unlabeled wifi for on-demand delivery. *Proceedings of the ACM on Interactive, Mobile, Wearable and Ubiquitous Technologies* 6, 2 (2022), 1–25.
- [19] Dongfang Guo, Chaojie Gu, Linshan Jiang, Wenjie Luo, and Rui Tan. 2022. Illoc: In-hall localization with standard lorawan uplink frames. *Proceedings of the ACM on Interactive, Mobile, Wearable and Ubiquitous Technologies* 6, 1 (2022), 1–26.
- [20] Jianlin Guo, Shuai Wang, Pu Wang, Kieran Parsons, Philip Orlit, Yukimasa Nagai, and Takenori Sumi. 2023. Active Cross-Technology Neighbor Discovery. US Patent App. 17/657,460.
- [21] Toshinari Hayakawa, Norifumi Murai, and Takatoshi Sugiyama. 2019. GPS Calculated Distance Error Improvement by Planar Approximation of Pseudo Range in Many Skyscrapers Environments. In *2019 IEEE 90th Vehicular Technology Conference (VTC2019-Fall)*. IEEE, 1–5.
- [22] Wenchao Jiang, Zhimeng Yin, Song Min Kim, and Tian He. 2016. Side channel communication over wireless traffic: A ctc design. In *Proceedings of the 14th ACM Conference on Embedded Network Sensor Systems CD-ROM*. 346–347.
- [23] Benjamin Kempke, Pat Pannuto, Bradford Campbell, and Prabal Dutta. 2016. Surepoint: Exploiting ultra wideband flooding and diversity to provide robust, scalable, high-fidelity indoor localization. In *Proceedings of the 14th ACM Conference on Embedded Network Sensor Systems CD-ROM*. 137–149.
- [24] Manikanta Kotaru, Kiran Joshi, Dinesh Bharadvia, and Sachin Katti. 2015. Spotfi: Decimeter level localization using wifi. In *Proceedings of the 2015 ACM conference on special interest group on data communication*. 269–282.
- [25] Hang Li, Xi Chen, Ju Wang, Di Wu, and Xue Liu. 2021. DAFI: WiFi-based device-free indoor localization via domain adaptation. *Proceedings of the ACM on Interactive, Mobile, Wearable and Ubiquitous Technologies* 5, 4 (2021), 1–21.
- [26] Zhijun Li and Tian He. 2017. Webee: Physical-layer cross-technology communication via emulation. In *Proceedings of the 23rd Annual International Conference on Mobile Computing and Networking*. 2–14.
- [27] Jun Liu, Jiayao Gao, Sanjay Jha, and Wen Hu. 2021. Seirios: leveraging multiple channels for LoRaWAN indoor and outdoor localization. In *Proceedings of the 27th Annual International Conference on Mobile Computing and Networking*. 656–669.
- [28] Jinyi Liu, Wenwei Li, Tao Gu, Ruiyang Gao, Bin Chen, Fusang Zhang, Dan Wu, and Daqing Zhang. 2023. Towards a dynamic fresnel zone model to wifi-based human activity recognition. *Proceedings of the ACM on Interactive, Mobile, Wearable and Ubiquitous Technologies* 7, 2 (2023), 1–24.
- [29] Jinyi Liu, Youwei Zeng, Tao Gu, Leye Wang, and Daqing Zhang. 2021. WiPhone: Smartphone-based respiration monitoring using ambient reflected WiFi signals. *Proceedings of the ACM on Interactive, Mobile, Wearable and Ubiquitous Technologies* 5, 1 (2021), 1–19.
- [30] Ruofeng Liu, Zhimeng Yin, Wenchao Jiang, and Tian He. 2019. LTE2B: Time-domain cross-technology emulation under LTE constraints. In *Proceedings of the 17th Conference on Embedded Networked Sensor Systems*. 179–191.
- [31] Ruofeng Liu, Zhimeng Yin, Wenchao Jiang, and Tian He. 2021. WiBeacon: Expanding BLE location-based services via WiFi. In *Proceedings of the 27th annual international conference on mobile computing and networking*. 83–96.
- [32] Zhicheng Luo, Qianyi Huang, Rui Wang, Hao Chen, Xiaofeng Tao, Guihai Chen, and Qian Zhang. 2022. WISE: Low-cost wide band spectrum sensing using UWB. In *Proceedings of the 20th ACM Conference on Embedded Networked Sensor Systems*. 651–666.
- [33] Yongsen Ma, Yunze Zeng, and Vivek Jain. 2020. CarOSense: Car occupancy sensing with the ultra-wideband keyless infrastructure. *Proceedings of the ACM on Interactive, Mobile, Wearable and Ubiquitous Technologies* 4, 3 (2020), 1–28.
- [34] Gavin Marrow, Michael McLaughlin, and Ciaran McElroy. 2018. Measuring angle of incidence in an ultrawideband communication system. US Patent 10,075,210.
- [35] NXP. 2019. NXP and VW share the wide possibilities of Ultra-Wideband's (UWB) fine ranging capabilities, <https://www.nxp.com/company/about-nxp/nxp-and-vw-share-the-wide-possibilities-of-ultra-widebands-uwb-fine-ranging-capabilities-NW-VOLKSWAGEN-SHOWCASES-UWB>.
- [36] Pat Pannuto, Benjamin Kempke, Bradford Campbell, and Prabal Dutta. 2018. Indoor ultra wideband ranging samples from the DecaWave DW1000 including frequency and polarization diversity. In *Proceedings of the First Workshop on Data Acquisition To Analysis*. 11–12.
- [37] Shuang Qiao, Chenhong Cao, Haoquan Zhou, and Wei Gong. 2023. The trip to WiFi indoor localization across a decade—A systematic review. In *2023 26th International Conference on Computer Supported Cooperative Work in Design (CSCWD)*. IEEE, 642–647.
- [38] Zhenquan Qin, Mingyi Yang, Bingxian Lu, Lei Wang, and Jian Fang. 2019. ZiFi: A lightweight cross-technology communication via RSS encoding. In *Proceedings of the ACM SIGCOMM 2019 Conference Posters and Demos*. 112–113.
- [39] Qorvo. 2017. DW1000 Datasheet. <https://www.qorvo.com/products/p/DW1000> Accessed on July 30th, 2024.
- [40] Qorvo. 2020. DW 3000 Data Sheet. <https://www.qorvo.com/products/p/DW3220#documents> Accessed on October 31th, 2024.
- [41] Qorvo. 2020. DW3000 Datasheet, <https://www.qorvo.com/products/d/da008142>.
- [42] Yili Ren, Zi Wang, Sheng Tan, Yingying Chen, and Jie Yang. 2021. Winect: 3d human pose tracking for free-form activity using commodity wifi. *Proceedings of the ACM on Interactive, Mobile, Wearable and Ubiquitous Technologies* 5, 4 (2021), 1–29.
- [43] Yili Ren, Zi Wang, Yichao Wang, Sheng Tan, Yingying Chen, and Jie Yang. 2022. Gopose: 3d human pose estimation using wifi. *Proceedings of the ACM on Interactive, Mobile, Wearable and Ubiquitous Technologies* 6, 2 (2022), 1–25.

- [44] NXP Semiconductors. 2021. Determine a Device's Relative Position with UWB Localization Capability. <https://www.nxp.com/applications/enabling-technologies/connectivity/ultra-wideband-uwb:UWB>.
- [45] Junyang Shi, Di Mu, and Mo Sha. 2021. Enabling cross-technology communication from LoRa to ZigBee via payload encoding in sub-1 GHz bands. *ACM Transactions on Sensor Networks (TOSN)* 18, 1 (2021), 1–26.
- [46] Elahe Soltanaghaei, Adwait Dongare, Akarsh Prabhakara, Swarun Kumar, Anthony Rowe, and Kamin Whitehouse. 2021. Tagfi: Locating ultra-low power wifi tags using unmodified wifi infrastructure. *Proceedings of the ACM on Interactive, Mobile, Wearable and Ubiquitous Technologies* 5, 1 (2021), 1–29.
- [47] Mert Torun and Yasamin Mostofi. 2023. Wi-Flex: Reflex Detection with Commodity WiFi. *Proceedings of the ACM on Interactive, Mobile, Wearable and Ubiquitous Technologies* 7, 3 (2023), 1–27.
- [48] Raghav H Venkatnarayan, Muhammad Shahzad, Sangki Yun, Christina Vlachou, and Kyu-Han Kim. 2020. Leveraging polarization of WiFi signals to simultaneously track multiple people. *Proceedings of the ACM on Interactive, Mobile, Wearable and Ubiquitous Technologies* 4, 2 (2020), 1–24.
- [49] Haoyu Wang, Jiazhao Wang, Wenchao Jiang, Shuai Wang, and Demin Gao. 2024. Physical Layer Cross-Technology Communication Via Explainable Neural Networks. *IEEE Transactions on Mobile Computing* (2024).
- [50] Shuai Wang, Jianlin Guo, Pu Wang, Kieran Parsons, Philip Orlik, Yukimasa Nagai, Takenori Sumi, and Parth Pathak. 2022. X-disco: Cross-technology neighbor discovery. In *2022 19th Annual IEEE International Conference on Sensing, Communication, and Networking (SECON)*. IEEE, 163–171.
- [51] Shuai Wang, Woojae Jeong, Jinhwan Jung, and Song Min Kim. 2020. X-MIMO: Cross-technology multi-user MIMO. In *Proceedings of the 18th Conference on Embedded Networked Sensor Systems*. 218–231.
- [52] Shuai Wang, Song Min Kim, and Tian He. 2018. Symbol-level cross-technology communication via payload encoding. In *2018 IEEE 38th International Conference on Distributed Computing Systems (ICDCS)*. IEEE, 500–510.
- [53] WIKIPEDIA. 2024. List of UWB-enabled mobile devices. https://en.wikipedia.org/wiki/List_of_UWB-enabled_mobile_devices Accessed on July 30th, 2024.
- [54] WIKIPEDIA. 2024. List of WLAN channels. https://en.wikipedia.org/wiki/List_of_WLAN_channels Accessed on July 30th, 2024.
- [55] Han Xu, Zheng Yang, Zimu Zhou, Longfei Shangguan, Ke Yi, and Yunhao Liu. 2016. Indoor localization via multi-modal sensing on smartphones. In *Proceedings of the 2016 ACM International Joint Conference on Pervasive and Ubiquitous Computing*. 208–219.
- [56] Jing Yang, BaiShun Dong, and Jiliang Wang. 2022. VULoc: Accurate UWB localization for countless targets without synchronization. *Proceedings of the ACM on Interactive, Mobile, Wearable and Ubiquitous Technologies* 6, 3 (2022), 1–25.
- [57] Xuehan Ye, Shuo Huang, Yongcai Wang, Wenping Chen, and Deying Li. 2019. Unsupervised localization by learning transition model. *Proceedings of the ACM on Interactive, Mobile, Wearable and Ubiquitous Technologies* 3, 2 (2019), 1–23.
- [58] Yanzhen Ye, Bang Wang, Xianjun Deng, and Laurence T Yang. 2017. On solving device diversity problem via fingerprint calibration and transformation for RSS-based indoor localization system. In *2017 IEEE SmartWorld, Ubiquitous Intelligence & Computing, Advanced & Trusted Computed, Scalable Computing & Communications, Cloud & Big Data Computing, Internet of People and Smart City Innovation (SmartWorld/SCALCOM/UIC/ATC/CBDCom/IOP/SCI)*. IEEE, 1–8.
- [59] Enze Yi, Fusang Zhang, Jie Xiong, Kai Niu, Zhiyun Yao, and Daqing Zhang. 2024. Enabling WiFi Sensing on New-generation WiFi Cards. *Proceedings of the ACM on Interactive, Mobile, Wearable and Ubiquitous Technologies* 7, 4 (2024), 1–26.
- [60] Jin Zhang, Yuyan Dai, Jie Chen, Chengwen Luo, Bo Wei, Victor CM Leung, and Jianqiang Li. 2023. SIDA: Self-Supervised Imbalanced Domain Adaptation for Sound Enhancement and Cross-Domain WiFi Sensing. *Proceedings of the ACM on Interactive, Mobile, Wearable and Ubiquitous Technologies* 7, 3 (2023), 1–24.
- [61] Xianan Zhang, Lieke Chen, Mingjie Feng, and Tao Jiang. 2022. Toward reliable non-line-of-sight localization using multipath reflections. *Proceedings of the ACM on Interactive, Mobile, Wearable and Ubiquitous Technologies* 6, 1 (2022), 1–25.
- [62] Minghui Zhao, Tyler Chang, Aditya Arun, Roshan Ayyalasomayajula, Chi Zhang, and Dinesh Bharadia. 2021. Uloc: Low-power, scalable and cm-accurate uwb-tag localization and tracking for indoor applications. *Proceedings of the ACM on Interactive, Mobile, Wearable and Ubiquitous Technologies* 5, 3 (2021), 1–31.
- [63] Renjie Zhao, Pengyu Zhang, Yunfei Ma, and Xinyu Zhang. 2022. Ultra-wideband backscatter towards general passive iot localization. In *Proceedings of the 20th ACM Conference on Embedded Networked Sensor Systems*. 857–858.